Diogo, Antonia Cinira M.; Soares, Juliana G. M.; Albright, Thomas D.; Gattass, Ricardo

Two-dimensional map of direction selectivity in cortical visual area MT of Cebus monkey

Two-dimensional map of direction selectivity in cortical visual area MT of *Cebus* monkey*

ANTONIA CINIRA M. DIOGO[1], JULIANA G. M. SOARES[1],
THOMAS D. ALBRIGHT[2] and RICARDO GATTASS[1]

[1]Instituto de Biofísica Carlos Chagas Filho, UFRJ, 21941-900 Rio de Janeiro, RJ, Brazil
[2]Salk Institute, #10010 N. Torrey Pines Rd., La Jolla, California, 92037-1099, USA

ABSTRACT

We studied the spatial organization of direction of motion in visual area MT of the *Cebus apella* monkey. We used arrays of 6 (700 μm apart) parallel electrodes in penetrations tangential to the cortical layers to record multi-unit responses to moving bars, at 200 μm steps. We determined the direction selectivity at each recording site. The data from single penetrations showed cyclic and gradual changes in the direction selectivity of clusters of cells, intermixed with abrupt 180° discontinuities along the electrode track. In order to obtain maps of direction of motion selectivity, we examined the spatial distribution of direction of motion in MT and we applied a method to determine the location of the centers of radial arrangements of direction selectivity. This tangential organization is characterized by slow continuous changes in direction of motion, interrupted by discontinuities. The changes in direction selectivity are organized radially in a pinwheel fashion and in slabs of linear variation. The pinwheel arrangements have 800-1400 μm in diameter. The size of the radial arrangement is comparable to the point image size in area MT at each eccentricity.

Key words: extrastriate cortex, visual system, primates, direction of motion.

INTRODUCTION

The modular organization of the neocortex has been widely studied for decades. A characteristic feature of neocortical organization is the arrangement of neurons representing similar attributes into columns that extend from the cortical surface to the white matter (Mountcastle 1957, Hubel and Wiesel 1962, 1968, 1974). Mountcastle (1957), using single-unit recordings in the somatic sensory cortex of cats,

found the first evidence for neo-cortical columnar organization. This functional segregation of neurons was later demonstrated in different cortical areas for other stimulus modalities. In the primary visual cortex of cats and monkeys, Hubel and Wiesel (1962, 1974) found that cells in the same vertical column in the cortex had the same orientation preference, while cells in adjacent columns had preferences that differed slightly. The preferred orientation changed linearly as a function of distance through the cortex. A single 180°-cycle of orientation change encompass 500-700 μm of cortex. Linear orientation sequences were often interrupted by reversals in direction of motion or by discontinuous jumps up to 90°. The two-dimensional pattern of orientation se-

lectivity was not clear. Based on one-dimensional evaluation of orientation, Hubel and Wiesel (1974) suggested that the orientation preference might be represented in parallel slabs in primate visual cortex. Conventional microelectrode measurements offer a one-dimensional picture of columnar organization within a three-dimensional cortex; however, it has been difficult to deduce from such measurements the precise form of the larger two-dimensional (2D) columnar representation (Braitenberg and Braitenberg 1979).

Optical imaging of intrinsic signals offers an alternative and more direct means to assess the 2D topography of cortical columns. It has provided an elegant resolution to long-standing debates about the orientation column system of V1 (Blasdel and Salama 1986). Although revealing large-scale 2D columnar structure, there are some critical limitations to the optical imaging approach. One obvious problem is that optical signals cannot be recorded readily from cortical regions that are buried within sulci. Long before the description of the organization of these columns by the optical imaging method, Braitenberg and Braitenberg (1979), based on the analysis of published data on the orientation selectivity in V1 of cat (Albus 1975) and monkey (Hubel and Wiesel 1974), proposed that the orientation columns most probable were organized in radial arrangements. These authors, based on the analysis of published data from penetration oblique to the cortical surface, proposed a model for the geometry of the orientation columns in visual cortex. They showed that it was possible to reconstruct the arrangement of the orientation columns from long and sometimes multiple parallel penetrations if the tangential organization of the orientation was arranged radially around centers.

The goal of this study was to explore the tangential organization of direction of motion selective cells in MT in *Cebus apella*, using the Braitenberg's method. Area MT in *Cebus* is homologous to area MT of Old World macaque monkey (Fiorani et al. 1989, Gattass and Gross 1981). In *Cebus*, MT is an oval area mainly located in the posterior bank of

the dorsal portion of the superior temporal sulcus. Our approach involves the use of multiple microelectrodes that are arranged in linear arrays. The array enables a two-dimensional sampling of neuronal direction selectivity along each electrode and simultaneously across all electrodes of the array. We describe the modular 2D organization of direction-of-motion selectivity using the Braitenberg's method (Braitenberg and Braitenberg 1979) to reveal the centers of radial arrangements and to estimate their dimensions. A preliminary account of these results was presented previously in abstract form (Diogo et al. 1999).

MATERIALS AND METHODS

Three adult *Cebus* monkeys (*Cebus apella*) weighing between 2 and 3 Kg were recorded, 3-5 times each. All experimental protocols followed NIH guidelines for animal care and use and were approved by the Institutional Animal Care and Use Committee of the IBCCF/UFRJ.

ANIMAL PREPARATION AND MAINTENANCE

One week prior to the first recording session, a stainless steel cylinder and a head bolt, oriented in the stereotaxic planes, were affixed to the animal's skull with screws and dental acrylic. Surgical procedures were performed under aseptic conditions using ketamine anesthesia (20 mg/kg). For the recording sessions, animals were anesthetized initially using ketamine (20 mg/kg) followed by halothane 2.0% in a mixture of nitrous oxide and oxygen (7:3). They were paralyzed by a continuous infusion of pancuronium bromide (0.1 mg/kg/h), and artificially ventilated. Halothane was discontinued once paralysis became stable and anesthesia was maintained by a mixture of N_2O/O_2 (7:3) and by continuous infusion of phentanil citrate (0.003 mg/kg/h). Body temperature was maintained at 37-38°C with a heating pad, and the respiratory parameters were adjusted to give an end-tidal carbon dioxide level of about 4%. The head of the monkey was held firmly in a stereotaxic apparatus by means of the head bolt. There was

an intervening period of at least one week between successive recording sessions. Before visual stimulation began, the cornea was fitted with a contact lens and accommodation paralyzed by topical application of atropine (1%). The contra-lateral eye was focused on a tangent screen at a distance of 57 cm and the ipsilateral eye was occluded.

Recording sessions generally continued for 12-16 h. One hour before the end of recording session, the paralytic agent was discontinued. The recording cylinder was washed out and filled with saline and the animal allowed to recover. Usually within 3 h the animal was alert and active in his home cage.

Electrophysiological Recording

We used an array contained six parallel varnish-coated tungsten microelectrodes to record from clusters of cells in MT, in 200 μm steps. At each position of the microelectrode array, neuronal responses were assessed on each electrode. Visual stimuli were presented manually using a hand-held projector and a rear-projection screen. Patterns of stimulus selectivity recorded on each electrode were characterized by the experimenter, based on audio evaluation of firing rate under different conditions. After the neuronal receptive field (RF) boundaries were mapped, the preferred direction was determined by judging the best multi-unit response to a bar that was moved in systematically varied directions. If the site exhibited no strong responses compared to spontaneous activity, in all tested directions, it was classified as non-responsive. If the site was responsive to moving stimuli but had no clear direction preference, it was classified as pan-directional. Some recording sites had two preferred directions that were clearly better than the others. In such cases, we determined the preferred direction to be the one eliciting stronger responses. Recordings in these three animals were confined to the cortex representing an area of the visual field within approximately 10° of the fovea. Microelectrode array penetrations were approximately tangential (10-13°) to the surface of area MT. For all experiments, the relative position of the electrodes within the array was known precisely at the begin-

ning of each penetration. Electrolytic lesions (4 μA, 10 s) were used to mark the end of the penetrations.

Histology

At the end of a 3-5 weeks recording period, each animal was anesthetized with an overdose of sodium pentobarbital and perfused through the heart with saline followed by formalin solution. The brain was removed from the skull and sectioned at an angle 28° backward of the frontal plane. Sections were cut at 40 μm thickness. Alternate sections were stained for myelin by the Gallyas' (1979) method and for cell bodies, by a Nissl stain. The boundaries of area MT were determined based on characteristic myeloarchitecture (Ungerleider and Mishkin 1979, Gattass and Gross 1981, Van Essen et al. 1981). Microelectrode tracks and the location of the recording sites were reconstructed from the positions of electrolytic lesions. Data analysis was restricted to recording sites located in the heavily myelinated region along the floor and lower bank of the superior temporal sulcus.

The angle of the penetration in the plane of section was measured relative to the radial fascicles of fibers within the cortex. The angle of the penetration in the plane orthogonal to the plane of section was calculated by reconstructing the cortical surface from serial sections and estimating its slope.

Functional Maps of Motion Selectivity

The 2D functional organization of motion selectivity in MT was revealed by maps derived from a set of recordings with RF properties. Maps were constructed for both preferred direction of motion and preferred axis of motion. For unidirectional recording sites, preferred axis of motion was calculated directly from the preferred direction. For bi-directional recording sites, preferred axis of motion was defined as the smaller angle (i.e. $< 180°$) of the two preferred directions.

Using information derived from the reconstructed microelectrode penetrations, measurements of preferred direction were projected onto representations of the 2D cortical surface of area

MT. Oriented arrows represented preferred direction of motion at each recording site; preferred axis of motion was represented in the map by oriented bars. Asterisks were used to represent pan-directional recording sites. Non-responsive recording sites were excluded from the maps.

THE BRAITENBERG'S METHOD

We estimate the location of the centers of radial arrangements of direction of motion using the Braitenberg's method. Braitenberg and Braitenberg (1979) have proposed a simple method to uniquely define the position of these centers on the vicinity of the electrode tracks. Their method was based on the extension of successive oriented lines corresponding to the orientation selectivity at each recording site along an electrode track. We applied their method to the map of directional selectivity by plotting a line (2 mm long) orthogonal to the axis-of-motion selectivity. Using this method, we reconstructed the plane of penetration of the parallel electrode arrays using the gliosis, the linear cuts caused by the penetration of the electrode and the electrolytic lesions as landmarks in the histological sections. Then, we precisely locate the recording sites onto area MT to draw, at that location, a vector corresponding to the direction of motion, at the appropriate angle. Finally, we plot a 2 mm line orthogonal to the direction vector passing through the recording site. As shown in Figure 1, this method is a generalization of the Braitenberg's method for orientation.

Figures 1A and 1B show the graphical representation used by Braitenberg and Braitenberg (1979) to determine the location of the centers of the pinwheel. There is a strict spatial relationship between the angle of electrode track in the 2D surface and the representation of orientation, at each point. In Figure 1A, the Braitenberg line does not converge at the center of circular arrangement inasmuch as the angle of the electrode track is plotted at an inappropriate angle. The orientation map has a representation of the absolute angle of the stimulus in the visual field plotted in trigonometric space (0° to the right, 90° to the top, 180° to the left and

270° to the bottom). The appropriate angle of the penetration is the exact projection of the penetration track onto the cortical surface corresponding to the orientation map. In Figure 1B, the orientation selectivities of the receptive fields are the same ones as in Figure 1A, but the angle of the penetrations in relation to orientation map in the cortex is the appropriate one. The location of the bars in the penetration track is the same as in Figure 1A, but their orientation matches the orientation selectivity of the visual receptive field. Under this condition, it is possible to reconstruct the tangential map of orientation selectivity of the cortex and to reveal the location of the pinwheels. Figure 1D is a schematic diagram of the definition of the Braitenberg line for direction selectivity. In this portion of the figure, a 2 (two) mm line orthogonal to the direction of motion, passing through the recording site location allows the reconstruction of the direction of motion map and the location of the center of the pinwheels (Fig. 1E). As shown by Blasdel and Salama (1986) there are two types of pinwheels, with four possible configuration: centripetal, centrifugal, radial clockwise and radial counterclockwise. Thus for each pinwheel, the angle of the Braitenberg's line could be either orthogonal or co-linear with the axis of motion selectivity. This method is appropriate to reveal axis of motion maps and it is immune to fractures of direction of motion. The invariance to opposite direction of motion may suggest that direction of motion selectivity is organized later in the development of neural circuits in area MT.

Figure 1C shows a reconstruction of a pinwheel in the direction of motion map in an ideal sampling condition, using a very dense electrode array. The application of the Braitenberg's method to this simulated data allows the reconstruction of a circular arrangement of direction of motion, with no discontinuity. The dense sampling in this case allows a direct visualization of the direction of motion circular module. Figure 1F is a simulation of the use of an array similar to the one used in this study with recording sites spaced by 200 μm. In this case the application of the Braitenberg's method allow to re-

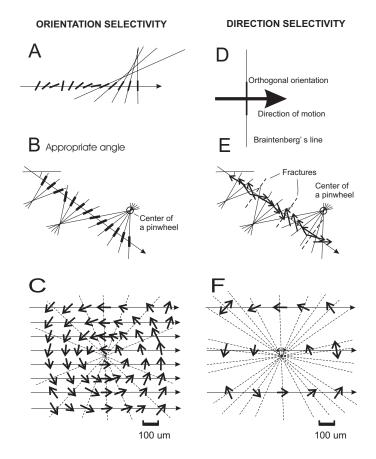**ORIENTATION SELECTIVITY**

DIRECTION SELECTIVITY

Fig. 1 – The method of Braitenberg (for details see text).

veal the center of a pinwheel which is not easy to detect by direct visualization.

We suspected of 2D-circular arrangements of direction of motion in our data because the changes of direction of motion were variable from one penetration to the other, and they followed certain patterns: there are portions with no change in direction selectivity; there are changes with different rates of axis of motion selectivity; and finally, a plot of axis of motion vs. distance consist of sigmoid segments, spanning for about $800 - 1400\,\mu$m. As shown by Braitenberg and Braitenberg (1979), electrode penetrations passing through the center of a pinwheel show no change in direction selectivity. Otherwise, the closer the electrode track is to the center of the pinwheel, larger the rate of change of axis of motion

per unit of distance traveled. Both in own data, as well as in Albright et al. (1984) data, the plot of axis of motion in degrees vs. distance consist of sigmoid segments, either ascending (clockwise rotation) or descending (counterclockwise ones) on the ordinate representing axis of motion. When two consecutive ascending (or descending) sigmoid segments appear in a penetration they are separated by a fracture or a jump in the plot.

RESULTS

Four hundred and thirty-two multi-unit recording sites were studied in tangential multi-electrode penetrations through area MT in three animals. In these animals were made qualitative assessment of RF properties, which involved manual presentation of

moving bars and experimenter judgments of the neuronal response as reproduced on an audio monitor. Among neuronal recording sites, 79% responded to moving stimuli. Ninety-three percent of the responsive sites, in turn, exhibited directional selectivity; the remaining responsive sites were pan-directional.

Recording Site Localization

We reconstructed electrode tracks in oblique frontal sections (sliced at an angle intended to match the plane of electrode penetrations), in conjunction with the positions of electrolytic lesions and myeloarchitectonic borders within the cortex, to provide evidence for the portion of each electrode trajectory that passed through area MT. Along these trajectories we localized the recording sites in the maps of directional preference. When the plane of section did not corresponded precisely to the plane of the electrode tracks, and thus each electrode array penetration traversed only a portion of a given section, we reconstructed a virtual plane of section using the location of the horizontal pins as alignment points and the portions of the sections containing the tracks of the penetrations as data. Gliosis from the penetrations, which progressed dorso-ventrally through the brain, can be used to draw the electrode tracks in MT. Electrolytic lesions made at the end of the penetrations are also used as depth marks. Figure 2B is a schematic representation of the reconstructed tracks (P1 and P2) of the penetration of two electrode arrays in Case 2.

Discrete Functional Maps Derived from RF Measurements

Two-dimensional maps of direction-of-motion and axis-of-motion preference are illustrated in Figures 3 and 4, respectively. These maps were derived from 108 "hand-mapped" measures of directional preference at each recording site along three multi-electrode penetrations made in Case 2. Visualization of ordered columnar arrangements in area MT was often facilitated by examining preferred axis of motion, rather than preferred direction of motion, because abrupt directional reversals disappears in this type of representation (see Albright et al. 1984).

Maps of Direction-of-motion Preference

Figure 3 contains two direction-of-motion maps obtained from area MT in Case 2. One of these maps (Figure 3A) was derived from multi-unit RF measurements made along one of the six-electrode array penetrations (P1) made in this animal. The second map (Figure 3B) covers the same patch of cortex represented in Figure 3A, but it is a "composite" derived from the fortuitous overlap of two array penetrations (P1 and P2). The locations of the two array penetrations relative to sulcal topography are indicated in Figure 2. Penetrations passing through MT were approximately tangential (5°) to the surface of this area. Preferred direction of motion values at each recording site have thus been projected directly onto a flat rectilinear representation of the cortical surface in each map, and are indicated by arrows. Significant map features revealed by comparison of selectivity along the electrodes are highlighted in each map by elongated rectangles and circles.

The map illustrated in Figure 3A, which was derived from the first array penetration (P1), contains notable sequences (bands) of regular linear progression (B1-B5), two of which cycle 180° or more (B3 and B4). This type of "sequence regularity" closely matches that seen along single electrode penetrations in macaque MT (Albright et al. 1984). As shown in Figure 2, the second array penetration (P2) happened to traverse a region of area MT that was also mapped by P1. The combined data set representing the intersection of these two arrays is shown in Figure 3B. Although we must assume a small amount of error in the alignment of reconstructed arrays, recording sites at the points of intersection between the two arrays exhibited remarkably consistent preferences (e.g. the two points of intersection of P2 with sequence B5 of P1). The 2D array, however, reveals additional map features undetectable from any single electrode. Consider, for instance, the pattern that emerges from three adjacent electrodes in the right portion of the map. In the region delimited by the circle (R1), diametri-
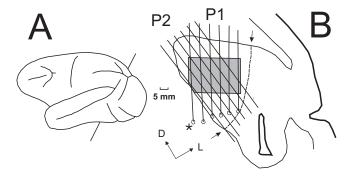
Fig. 2 – Oblique frontal sections (B), at the level indicated in the lateral reconstruction of the hemisphere (A). Arrows indicate the borders of MT. Electrode tracks are indicated by vertical and oblique lines. The boundaries of area MT were determined based on myeloarchitecture. The asterisc indicate the array of penetration with electrolitic lesions at the end of the electrode track.

cally opposed recording sites exhibited roughly parallel axis-of-motion selectivity. This arrangement suggests a radial pattern for axis-of-motion, which resembles a pinwheel with a diameter of approximately 1.4 mm. Comparisons between adjacent electrodes suggest radial arrangements that encompass a full cycle of 180° (R2 and R3). More generally, the linear sequences and radial patterns (R3) identifiable from the P1 data set, receive confirmation from P2. Some additional features, such as the broad radial pattern R4, which is not confidently recognizable in either data set considered alone, emerge from the joint P1+P2 map in the axis of motion map (Figure 4). One significant consequence of these frequent direction discontinuities, detectable upon close examination of the maps, is the complete absence of continuous sequences spanning 360° or more. Not surprisingly, there were also no radial arrangements present with 360° of continuous variation; reversals were also present in all identified pinwheels.

MAPS OF AXIS-OF-MOTION PREFERENCE

Figure 4 contains one axis-of-motion map derived from the penetration of two arrays of parallel electrodes. The preferred axis-of-motion observed at

each site is represented by an oriented line segment. To facilitate comparisons between axis- and direction-of-motion maps, the locations of salient features (linear sequences and "pinwheels") that were identified in the direction-of-motion maps (Figure 3B) are indicated in Figure 4. As previously pointed out by Albright et al. (1984), the preferred direction maps reveal that gradual sequences of preferred axis of motion are commonly interspersed with 180° reversals in preferred direction of motion. Adjacent recording sites that exhibit such 180° directional discontinuities disappear in Figure 4.

CENTER OF PINWHEELS

Braitenberg and Braitenberg (1979), based on data from penetration oblique to the cortical surface, proposed a model for the geometry of the orientation columns in visual cortex. They showed that it was possible to reconstruct the arrangement of the orientation columns by assuming that the tangential organization of the orientation was arranged radially around centers. They also proposed a simple method to uniquely define the position of these centers on the vicinity of the electrode tracks. As shown in Figure 5, a systematic application of this simple rule allowed revealing several others possible pinwheels
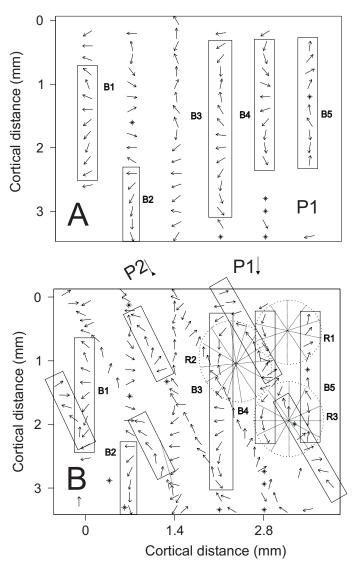
Fig. 3 – Patterns of direction-of-motion arrangement revealed by a manual study (hand plot) of receptive fields in P1 and P2. Small arrows show the direction-of-movement selectivity for each recording site. The ellipses (dotted) show radial arrangements or pinwheels (R1-R3), and the rectangles show linear arrangements in band (B1-B5). The panel in A is the result of the study in a recording plane with six simultaneously driven microelectrodes (P1). The lower panel (B) is a representation of the direction selectivity in two superposing oblique crossing planes (P1+P2). Note that each plane of penetration was reconstructed from successive 40 μm-thick oblique sections containing the electrode tracks. The reconstructed plane was treated as a single oblique plane containing the entire set of electrode tracks.
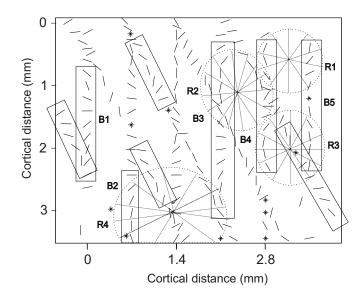
Fig. 4 – Patterns of axis-of-motion columns revealed by a manual plot of receptive field properties in two oblique crossing planes. Small bar shows the axis-of-movement selectivity for each recording site. The ellipses show radial arrangements or pinwheels and the rectangles show bands of linear arrangements. (See also legend for Figure 3).

not perceived previously, in Figure 3 or 4. Using a criterion of more than five intersections in a radius of 300 μm, we delineated additional pinwheels, adding to 13 pinwheels in 11,2 mm^2 of cortex. A systematic visual search for radial arrangements after the application of the Braitenberg' s method reveals that most of the pinwheels around the identified center could be seen in the raw data, if an educated observer could search for possible pinwheels arrangements long enough, or if he could adjust the direction selectivity within a range of half bandwith. Figure 5B is an artistic representation of the axis-of-motion map using the location and dimension of the radial arrangements suggested by the Braitenberg's method. In this figure, there are fewer discontinuities than in the direction map.

DISCUSSION

The reconstruction of the direction selectivity of neurons in planes of penetration of six parallel electrode arrays allowed us to reveal the two-dimensional organization of direction selectivity in MT of *Cebus* monkeys. The organization of direction selectivity showed an arrangement different from the regular ice-cube model proposed by Albright et al. (1984) for the organization of axis-of-motion in area MT of the macaque. The tangential organization of direction selectivity shows circular arrangements (pinwheels) separated by slow continuous changes in direction selectivity (slabs). These arrangements are similar to the ones previously described in cats V1 by Swindale et al. (1987) or in owl monkey area MT by Malonek et al. (1994).

COMPARISON WITH PREVIOUS STUDIES

We have applied this multielectrode array technology to the study of the columnar structure for motion processing in the middle temporal visual area (area MT) of primate visual cortex. Area MT is a visuotopically organized cortical region that receives direct input from area V1 (Ungerleider and Mishkin 1979, Gattass and Gross 1981, Van Es-
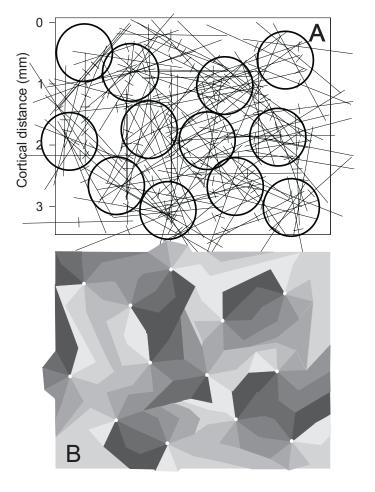
Fig. 5 – Pinwheels revealed by Braintemberg's method on the plane of penetration illustrated in Figures 3 and 4. The method is based on the extension of successive lines (2 mm long) orthogonal to the axis-of-motion selectivity at each recording site. In A we considered centers of radial arrangements (circles) the location that had more than five intersections in a radius of 200 μm. B is an artistic representation of the direction of motion map, where each half-tone density represents a range of 25 degrees.

sen et al. 1981). In macaques, where it has been studied most extensively, area MT lies in the lower bank and floor of the superior temporal sulcus along its posterior extent. This area contains a high proportion of directionally selective neurons and is believed to play a central role in visual motion processing (Zeki 1974, Albright et al. 1984, Maunsell and Van Essen 1983; see Albright 1993, for

review). Using the conventional electrophysiological approach (single microelectrode penetrations), Albright et al. (1984) demonstrated that neurons in area MT of *Macaca fascicularis* are organized into cortical columns of similar preferred direction and preferred axis-of-motion. The size of the hipercolumns for axis-of-motion (180° / 860 μm) is similar to that in macaque area V1 for orientation (Hubel

and Wiesel 1974). Although the one-dimensional (1D) electrophysiological data obtained by Albright et al. were insufficient to precisely identify the 2D columnar pattern in area MT, these investigators hypothesized a rectilinear arrangement of repeating direction and axis-of-motion columns, similar to the original "ice-cube" model for orientation and ocular dominance columns in area V1 (Hubel and Wiesel 1974).

Unfortunately, hypotheses regarding the 2D columnar pattern in area MT of macaques cannot be evaluated readily by optical imaging, inasmuch as MT is buried in a deep sulcus. However, electrophysiological evidence hinted that the owl monkey, which has a relatively flat cortex that is optically accessible, also possesses a direction column system (Baker et al. 1981). Malonek et al. (1994) used optical imaging of intrinsic neuronal signals to explore the functional architecture of owl monkey MT and they identified a columnar system for direction of motion. The 2D form of that system showed a clear tendency for radial organization, similar to the orientation column pinwheels of area V1.

Our use of multielectrode arrays has allowed us to advance beyond these findings in two important ways. Firstly, it has afforded an unprecedented opportunity to reveal the 2D pattern of direction columns in a primate species (*Cebus apella*) in which area MT is optically inaccessible. The pattern we have observed exhibits features that are characteristic of the pinwheel columnar systems seen in macaque V1 and owl monkey MT. Secondly our discovery of direction columns in the New World *Cebus* monkey has enabled us to document their remarkable resemblance to those of the Old World macaque, which suggests a common evolutionary adaptation.

Axis-of-motion Organization in Area MT

The study of the directional selectivity of multi-unit clusters in MT in Case 2, shown in Figure 3, indicated the existence of an organization for direction selectivity containing pinwheel-like circular modules and modules in bands or slabs. These arrangements consistently contain discontinuities. The direction preference changes smoothly, except at discontinuities. Two neighbors slabs varying in different way, one counterclockwise and the other one clockwise, can to generate a radial arrangement. Each half of one pinwheel can be a part of a slab. These two types of arrangement are intermixed and they overlap significantly. One possible interpretation is that they coexist and the 2D-organization of direction selectivity is a mosaic of slabs and pinwheels. However, another possibility is that each arrangement is an organizational consequence of the other. If we consider the axis-of-motion for each recording site and we substitute the directional selectivity by the axis-of-motion selectivity these arrangements become more clear with much less discontinuities. However, an axis-of-motion organization has probably limited biological meaning. An area where most of the neurons are responsive to moving stimuli and are unidirectional selective may play a role in the computation of trajectories of moving stimuli (Newsome et al. 1986) and the biological meaning of an object moving towards the animal is very different than that moving away from the animal. Inasmuch as the V1 projections to MT are topographically organized (Ungerleider and Desimone 1986, Sousa et al. 1991, Rosa et al. 1993) it is likely that regions selective to opposing direction to be close to each other in the map, although they may constitute portions of different functional modules.

Additional Inferences and Interpolations

The original proposal for the organization of the orientation columns in V1 (Hubel and Wiesel 1974) and for the directional columns in MT (Albright et al. 1984) were based on a regular and sequential superimposition of rectangular slabs adjacent to each other resembling an ice-cube tray. The study with arrays of parallel electrodes distant 700 mm from each other provide a coarse matrix not suitable for interpolation of directional selectivity inasmuch as most of the circular arrangements described in other visual areas had a size smaller than the resolution in one dimension of the map. In addition, the observa-

tion of abrupt shifts or discontinuities in the 2D-map made circular interpolation of direction selectivity inappropriate for such course matrices. Arrays with smaller inter-electrode distances and larger numbers of electrodes are currently being used in conjunction with an automatic data acquisition system to allow proper interpolation of cellular activity and of RF properties in *Cebus* visual area MT.

The Braitenberg's Method

The analysis of the data of one penetration of the 6-electrode array like the one in Figure 3A allows to identify bands of linear variation (B1-B5) and perhaps proposes the location of three possible circular arrangement or pinwheels (later labeled R1-R3 in Figure 3B). By adding another penetration of the array at the same plane of P1 tilted 30 degrees medial at the oblique posterior plane, the spatial sampling increases and it is possible to identify the location of at least four pinwheels (R1-R4). With more data points at the penetration plane, we are able to see more evidence for additional circular arrangements. However, with the systematic application of the Braitenberg's method, with the criteria of five lines converging in a circle of 300μm, we were able to locate the center of 13 pinwheels in a patch of cortex of $3.2 \times 3.5 \mu$m. The size of these circular patches was estimated to be 900-1000 μm in diameter, which is comparable to the size of the point image size in MT.

Modular Organization and Visual Topography

The search for models for visual processing with repetitive modulus has brought basic topographical definitions of properties and of patches underlying the process of decoding of physical parameters of the visual stimuli. The definitions of receptive field size, cortical magnification factor and point image size (Gattass et al. 1990 for review) are useful to define the maps of visual topography of an area. MT in *Cebus* has point images of about 1 mm in diameter, virtually invariant with eccentricity (Fiorani et al. 1989). Figure 6 shows a representation of the

visual topography of MT in *Cebus* and its relation to circular arrangements (pinwheels) of direction selectivity and to point image sizes. Surprisingly, the size of a point image, that is the area of the cortex influenced by a moving point in the visual fields, is very similar to the size of the pinwheels that we are proposing for area MT of *Cebus*. Currently, we have no data on the spatial relationship of these two modules. If they are independent, partially, or completely overlapped are still issues requiring further systematic investigations.
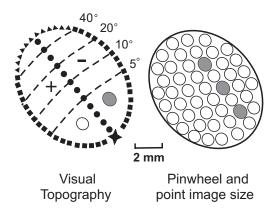

Fig. 6 – Visual map of MT and dimensions of point image size (gray circle) and radial arrangements (open circle) of direction selectivity. Star, foveal representation; black squares, vertical meridian; filled circles, horizontal meridian; dashed lines, iso-eccentricity lines; triangles, periphery.

RESUMO

Estudamos a organização espacial da seletividade ao sentido do movimento na área visual MT do macaco *Cebus apella*. Utilizamos um arranjo de 6 eletródios paralelos (separados por 700μm) em penetrações tangenciais às camadas corticais para registrar, a cada 200μm, a atividade multi-unitária em resposta a barras em movi-

mento. Determinamos a seletividade ao sentido de movimento em cada sítio de registro. Os dados captados por um único eletródio mostraram uma mudança cíclica e gradual na seletividade ao sentido de movimento dos grupos de neurônios registrados ao longo da trajetória do eletródio, interrompida por mudanças abruptas de 180° ocasionando descontinuidades na seletividade ao sentido do movimento. Para obter mapas de seletividade ao sentido do movimento, examinamos a distribuição espacial da seletividade ao sentido do movimento e aplicamos um método para determinar a localização dos centros dos arranjos radiais formados pela seletividade ao sentido de movimento. Esta organização tangencial é caracterizada por mudanças lentas e contínuas na seletividade ao sentido de movimento interrompida por descontinuidades. As mudanças na seletividade a sentido são organizadas radialmente formando cata-ventos (*pinwheels*) e bandas de variação linear. Os cata-ventos têm $800 - 1400\mu$m de diâmetro. A cada excentricidade, o tamanho desses arranjos radiais é comparável ao tamanho da imagem de um ponto na área MT.

Palavras-chave: Córtex extra-estriado, sistema visual, primatas, sentido de movimento.

REFERENCES

ALBRIGHT TD. 1993. Cortical processing of visual motion. Rev Oculomot Res 5: 177-201.

ALBRIGHT TD, DESIMONE R AND GROSS CG. 1984. Columnar organization of directionally selective cells in visual area MT of the macaque. J Neurophysiol 51: 16-31.

ALBUS K. 1975. A quantitative study of the projection area of the central and the paracentral visual field in area 17 of the cat II. The spatial organization of the orientation domain. Exp Brain Res 24: 181-202.

BAKER JF, PETERSEN SE, NEWSOME WT AND ALLMAN JM. 1981. Visual response properties of neurons in four extrastriate visual areas of the owl monkey (*Aotus trivigatus*): a quantitative comparison of medial, dorsomedial, dorsolateral, and middle temporal areas. J Neurophysiol 45: 397-416.

BLASDEL GG AND SALAMA G. 1986. Voltage-sensitive dyes reveal a modular organization in monkey striate cortex. Nature 321: 579-585.

BRAITENBERG V AND BRAITENBERG C. 1979. Geometry of orientation columns in the visual cortex. Biol Cybern 33:179-186.

DIOGO ACM, SOARES JGM, ALBRIGHT TD AND GATTASS R. 1999. Columnar organization of area MT in *Cebus apella*. Soc Neurosci Abs 25: 672.

FIORANI M, GATTASS R, ROSA MGP AND SOUSA APB. 1989. Visual area MT in the *Cebus* monkey: location, visuotopic organization, and variability. J Comp Neurol 287: 98-118.

GALLYAS F. 1979. Silver staining of myelin by means of physical development. Neurol Res 1: 203-209.

GATTASS R AND GROSS CG. 1981. Visual topography of the striate projection zone (MT) in posterior superior temporal sulcus of the macaque. J Neurophysiol 46: 621-638.

GATTASS R, ROSA MG, SOUSA APB, PINON MC, FIORANI M AND NEUENSCHWANDER S. 1990. Cortical streams of visual information processing in primates. Braz J Med Biol Res 23: 375-93.

HUBEL DH AND WIESEL TN. 1962. Receptive fields, binocular interaction and functional architecture in the cat's visual cortex. J Physiol Lond 160:106-154.

HUBEL DH AND WIESEL TN. 1968. Receptive fields and functional architecture of monkey striate cortex. J Physiol 195: 215-243.

HUBEL DH AND WIESEL TN. 1974. Sequence regularity and geometry of orientation columns in the monkey striate cortex. J comp Neurol 158: 267-293.

MALONEK D, TOOLTELL RBH AND GRINVALDI A. 1994. Optical imaging reveals the functional architecture of neurons processing shape and motion in owl monkey area MT. Proc R Soc Lond B 258: 109-119.

MAUNSELL JH AND VAN ESSEN DC. 1983. Functional properties of neurons in middle temporal visual area of the macaque monkey I. Selectivity for stimulus direction, speed and orientation. J Neurophysiol 49: 1127-1147.

MOUNTCASTLE VB. 1957. Modality and topographic properties of single neurons of cat's somatic sensory cortex. J Neurophysiol 20: 408-34.

NEWSOME WT, MAUNSELL JHR AND VAN ESSEN DC. 1986. Ventral posterior visual area of the macaque: Visual topography and areal boundaries. J Comp Neurol 252: 139-153.

ROSA MGP, SOARES JGM, FIORANI M AND GATTASS R. 1993. Cortical afferents of visual area MT in the *Cebus* monkey: Possible homologies between New and Old World monkeys. Visual Neurosci 10: 827-855.

SOUSA APB, PINON MC, GATTASS R AND ROSA MGP. 1991. Topographic organization of cortical input to striate cortex in the *Cebus* monkey: A fluorescent tracer study. J Comp Neurol 308: 665-682.

SWINDALE NV, MATSUBARA JA AND CYNADER MS. 1987. Surface organization of orientation and direction selectivity in cat area 18. J Neurosci 7: 1414-1427.

UNGERLEIDER LG AND DESIMONE R. 1986. Projections to the superior temporal sulcus from the central and peripheral field representations of V1 and V2. J. Comp Neurol 248: 147-163.

UNGERLEIDER LG AND MISHKIN M. 1979. The striate projection zone in the superior temporal sulcus of *Macaca mullata*: Location and topographic organization. J Comp Neurol 188: 347-366.

VAN ESSEN DC, MAUNSELL JHR AND BIXBY JL. 1981. The Middle Temporal visual area in the macaque: myeloarchitecture, connections, functional properties and topographic organization. J Comp Neurol 199: 293-326.

ZEKI SM. 1974. Functional organization of a visual area in posterior bank of the *Rhesus* monkey. J Physiol 236: 549-573.